Available online at www.sciencedirect.com
ScienceDirect
Ceramics International 37 (2011) 2837–2843
CERAMICS INTERNATIONAL
www.elsevier.com/locate/ceramint

Effect of oxygen partial pressure on the structural, optical and electrical properties of sputtered NiO films

A. Mallikarjuna Reddy [a], A. Sivasankar Reddy [b], Kee-Sun Lee [b], P. Sreedhara Reddy [a,*]

[a] Department of Physics, Sri Venkateswara University, Tirupati 517502, India
[b] Division of Advanced Materials Engineering, Kongju National University, Budaedong, Cheonan City, South Korea

Received 19 February 2011; received in revised form 28 April 2011; accepted 28 April 2011
Available online 5 May 2011

Abstract

Nickel oxide (NiO) thin films were deposited on glass substrates by dc reactive magnetron sputtering technique. The influence of oxygen partial pressure on the structural, microstructural, compositional, optical and electrical properties of NiO films was investigated by X-ray diffraction, scanning electron microscopy with energy dispersive spectroscopy, spectrophotometer and Hall effect studies. The XRD analysis showed that the preferred orientation changed from (2 0 0) to (2 2 0) as the oxygen partial pressure increases. Fine grains were observed at an oxygen partial pressure of 6×10^{-2} Pa. The deposited films exhibited optical transmittance of 60% and direct band gap of 3.82 eV at 6×10^{-2} Pa. The Hall measurements showed that the electrical resistivity of NiO films decreases as oxygen partial pressure increased to 6×10^{-2} Pa, thereafter increased at higher oxygen partial pressures.

Keywords: C. Electrical properties; Nickel oxide; Magnetron sputtering; Oxygen partial pressure

1. Introduction

Nickel oxide (NiO) is a wide band gap semiconductor with energy gap in the range of 3.6–4.0 eV [1] and exhibits excellent chemical stability. Because of its interesting optical, electrical and magnetic properties, it has immense potential in a number of applications. NiO is a p-type semiconductor with a wide range of applications such as transparent conductive films [2], spin-valve giant magneto (GMR) sensor [3–6], gas sensors [7], chemical sensors [8], electrochromic display devices [9], etc. NiO has a rock salt crystalline structure and has a lattice parameter 0.4176 nm. It is evident that the improvement of the material properties can be reached by the optimization of the preparation conditions. NiO films can be fabricated by different physical and chemical vapour deposition techniques and numerous attempts including sputtering [10,11], plasma-enhanced chemical vapour deposition [12], pulsed laser deposition [13], electrochemical deposition [14,15], sol–gel [16], and spray pyrolysis [17] have been used in the preparation NiO thin films. Among these methods, reactive sputtering is considered to be most widely useful technique having high deposition rates, uniformity over large areas of the substrates and easy control over the composition of the deposited films. The properties of the deposited films mainly depend on the deposition parameters such as substrate temperature, oxygen partial pressure, sputtering power, sputtering pressure and substrate bias voltage. In the present study, NiO thin films were deposited using dc reactive magnetron sputtering technique and studied the effect of oxygen partial pressure on the structural, microstructural, compositional, optical and electrical properties.

2. Experimental

NiO thin films were grown on Corning 7059 glass substrates by using the dc reactive magnetron sputtering from a homemade circular planar magnetron sputtering system. The sputtering system is capable of creating an ultimate vacuum of 5×10^{-4} Pa. The sputter chamber was pumped with diffusion pump and rotary pump combination. The pressure in the sputter chamber was measured using digital Pirani and Penning gauge combination. A circular planar magnetron of 100 mm diameter was used as the magnetron cathode. The magnetron target

* Corresponding author. Tel.: +91877 2289472; fax: +91877 2249611.
E-mail address: psreddy4@gmail.com (P.S. Reddy).

0272-8842/$36.00
doi:10.1016/j.ceramint.2011.04.121

assembly was mounted on the top of the sputter chamber such that the sputtering could be done by sputter down configuration. A continuously variable dc power supply of 1000 V and 1 A was used as a power source for sputtering. A 100 mm diameter and 3 mm thick pure nickel (99.98%) was used as sputter target. Pure argon was used as sputter gas and oxygen as reactive gas. The flow rates of both argon and oxygen gases were controlled individually by Tylan mass flow controllers. Before deposition of each film, the target was sputtered in pure argon atmosphere for 10 min to remove oxide layer if any on the surface of the target. NiO thin films were deposited at various oxygen partial pressures from 2×10^{-2} to 10×10^{-2} Pa by keeping the other deposition conditions such as substrate temperature, sputtering power and sputtering pressure as constant. The sputtering conditions maintained during the growth of NiO films are given in Table 1. The deposited films were characterized by studying crystallographic structure, morphological, optical and electrical properties. The crystallographic structure of the films was analyzed by X-ray diffractometer using Cu Kα radiation (λ = 0.1546 nm) of model 3033TT manufactured by Seifert. The surface morphology was studied by Scanning Electron Microscope (SEM) of model EVO MA 15 manufactured by Carl Zeiss, for which an EDS is attached of model Inca Penta FETx3 manufactured by Oxford Instruments was used for composition analysis. The optical properties of the films were carried out by Perkin Elmer Lambda 950 UV–Vis–NIR double beam spectrophotometer. The FTIR studies were carried out by using Perkin Elmer Spectrum 100 FTIR spectrometer. The electrical resistivity and Hall mobility were studied by employing the van der Pauw method [18].

The sheet resistance (ρ_s) of the films was calculated using the equation:

$$\rho_s = \left(\frac{\pi}{\ln_2}\right) f\left[\frac{(R_1 + R_2)}{2}\right] \quad (1)$$

where f is the van der Pauw correction factor, which depends on the position of electrical contacts on the film surface

$$f = \left(1 - \frac{\ln_2}{2}\right)\left[\frac{(R_1 - R_2)}{(R_1 + R_2)}\right]^2 \quad (2)$$

The electrical resistivity (ρ) of the films was determined from the relation

$$\rho = \rho_s \times t \quad (3)$$

Table 1
Deposition parameters maintained during the deposition of NiO films by dc reactive magnetron sputtering at various oxygen partial pressures.

Sputtering target pure nickel (99.98%)	100 mm diameter and 3 mm thick
Target to substrate distance	70 mm
Substrates	Corning 7059 glass
Ultimate pressure (P_U)	5×10^{-4} Pa
Oxygen partial pressure (pO_2)	2×10^{-2} to 10×10^{-2} Pa
Sputtering pressure (P_W)	4 Pa
Substrate temperature (T_S)	523 K
Sputtering power (S_p)	150 W

where t is the film thickness. The Hall mobility (μ) of the films was calculated from the relation

$$\mu = (\Delta R \times 10^8) B \rho_s \quad (4)$$

where ΔR is the change of resistance with the applied magnetic field (B).

3. Results and discussion

3.1. Deposition rate

The deposition rate of the films was directly influenced by the oxygen partial pressure maintained during the preparation of the films. The variation of deposition rate with the oxygen partial pressure was shown in Fig. 1. The deposition rate decreases from 22.7 to 8.1 nm/min as oxygen partial pressure increases from 2×10^{-2} to 10×10^{-2} Pa. At lower oxygen partial pressures the deposition rate was high due to the high sputtering yield of nickel and insufficient availability of oxygen for reaction with nickel. The decrease in deposition rate with oxygen partial pressure was due to the oxidation of sputter target resulting low sputtering yield. This type of dependence of deposition rate on the oxygen partial pressure was also observed in dc magnetron sputtered Cu_2O films [19].

3.2. Structural properties

The X-ray diffraction patterns of the NiO films formed at different oxygen partial pressures were shown in Fig. 2. The films were identified to be polycrystalline and retain rock salt structure. The films prepared at low oxygen partial pressure of 2×10^{-2} Pa exhibited (2 0 0) orientation. As the oxygen partial pressure increased to 4×10^{-2} Pa, the films exhibited (2 2 0) orientation along with (2 0 0), on further increasing the oxygen partial pressure to 6×10^{-2} Pa the intensity of the (2 2 0) peak

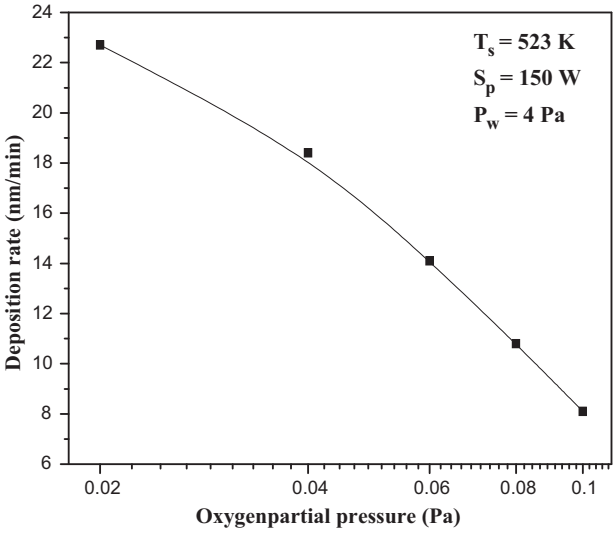

Fig. 1. Variation of deposition rate of NiO films as a function of oxygen partial pressure.

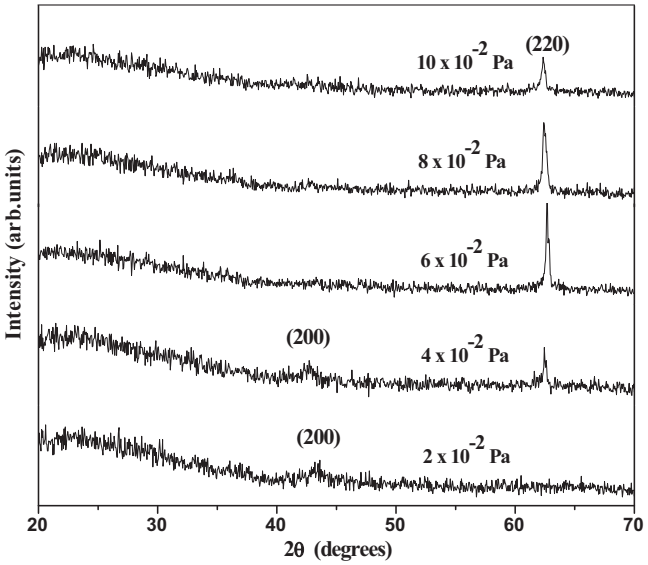

Fig. 2. X-ray diffraction patterns of NiO films at various oxygen partial pressures.

was increased and becomes sharper, and (2 0 0) peak was disappeared. With increasing the oxygen partial pressure, the mean free path of the atoms was changed, as a result the deposited atoms might have altered their direction, energy, momentum and mobility, this may be the reason for orientation change. Beyond this oxygen partial pressure, the intensity of the (2 2 0) peak was gradually decreased. At higher oxygen partial pressures, the excess oxygen might induce defects in the films, which influenced the nucleation and growth of the films, consequently the degradation of the crystalline quality. These results were in agreement with the results reported by Lee et al. [20], who observed that the decrease of crystallinity at higher oxygen partial pressure in dc reactive magnetron sputtered NiO films. Fujji et al. [21] was also reported the decrease in the intensity of (2 0 0) peak with increasing of oxygen partial pressure in dc magnetron sputtered NiO films. The increased intensity of the (2 2 0) peak with increasing the oxygen partial pressure up to 6×10^{-2} Pa may be due to an increase in the size of grains. By comparing between XRD and SEM results, it is apparent that the (2 2 0) peak of NiO films is related with the grain growth of the film. The lattice parameter of the films was also influenced by the oxygen partial pressure. The lattice parameter of the films was decreased from 0.4202 to 0.4189 nm with increasing the oxygen partial pressure up to 6×10^{-2} Pa, thereafter the lattice parameter was increased to 0.4207 nm at higher oxygen partial pressure of 10×10^{-2} Pa. The present obtained lattice parameter value of 0.4189 nm at 6×10^{-2} Pa was close to the standard value [JCPDS no: 78-0643].

The stress (σ) developed in the films was calculated from the X-ray diffraction data employing the relation [22]

$$\sigma = -E\frac{(a - a_o)}{2\nu a_o} \quad (5)$$

where E is the Young's modulus of the NiO (200 GPa), a is the lattice parameter of the bulk material, a_o is the measured lattice parameter and ν is the Poisson's ratio (0.31). The stress developed in the films is obtained by the shift in the interplanar spacing hence change in the lattice parameter. The tensile stress in the films decreased from 1.9961 to 1.0091 GPa with increasing oxygen partial pressure from 4×10^{-2} to 6×10^{-2} Pa, thereafter it increased to 2.3773 GPa at 10×10^{-2} Pa for (2 2 0) peak. The tensile stress developed in the films is due to the existence of microscopic voids incorporated in the films during condensation [23].

Table 2
Structural information of dc reactive magnetron sputtered NiO films at various oxygen partial pressures.

pO_2 (Pa)	Orientation	Lattice parameter (nm)	Grain size (nm)	Stress (GPa)
2×10^{-2}	(2 0 0)	0.4190	8.28	1.0778
4×10^{-2}	(2 2 0)	0.4202	28.29	1.9961
6×10^{-2}	(2 2 0)	0.4189	29.17	1.0091
8×10^{-2}	(2 2 0)	0.4203	22.17	2.0729
10×10^{-2}	(2 2 0)	0.4207	18.98	2.3773

The grain size (L) of the films was calculated for (2 2 0) peak by using Scherer's equation,

$$L = \frac{K\lambda}{\beta \cos\theta} \quad (6)$$

where K is the correction factor, λ is the wavelength of the incident beam, β is the full width at half maximum corresponding to diffraction angle θ.

The grain size of the films increased from 28.29 nm to 29.17 nm with the increase of oxygen partial pressure from 4×10^{-2} to 6×10^{-2} Pa, thereafter it decreased to 18.98 nm with increase of oxygen partial pressure to 10×10^{-2} Pa. The decreasing of the grain size was attributed to the segregation of oxygen into the grain boundaries, which causes limited grain boundary mobility, and therefore a decrease in grain size [24]. The lattice parameter, grain size and stress of the NiO films as a function of oxygen partial pressure were given in Table 2.

3.3. Surface microstructure and composition

The scanning electron microscopy images of NiO films deposited at various oxygen partial pressures were shown in Fig. 3. Very smooth and uniform surface was observed at an oxygen partial pressure of 2×10^{-2} Pa and the fine and uniform grains were appeared when the films deposited at oxygen partial pressure of 6×10^{-2} Pa. The size of the grains decreased when the films deposited beyond this oxygen partial pressure. The Energy Dispersive Spectroscopy (EDS) was employed to identify the composition of the as deposited NiO films at different oxygen partial pressures. Fig. 4 shows the EDS spectra of NiO films deposited at various oxygen partial pressures. EDS results revealed that all the deposited films consists of nickel and oxygen and the composition of the films was varied with oxygen partial pressure (Table 3) and the

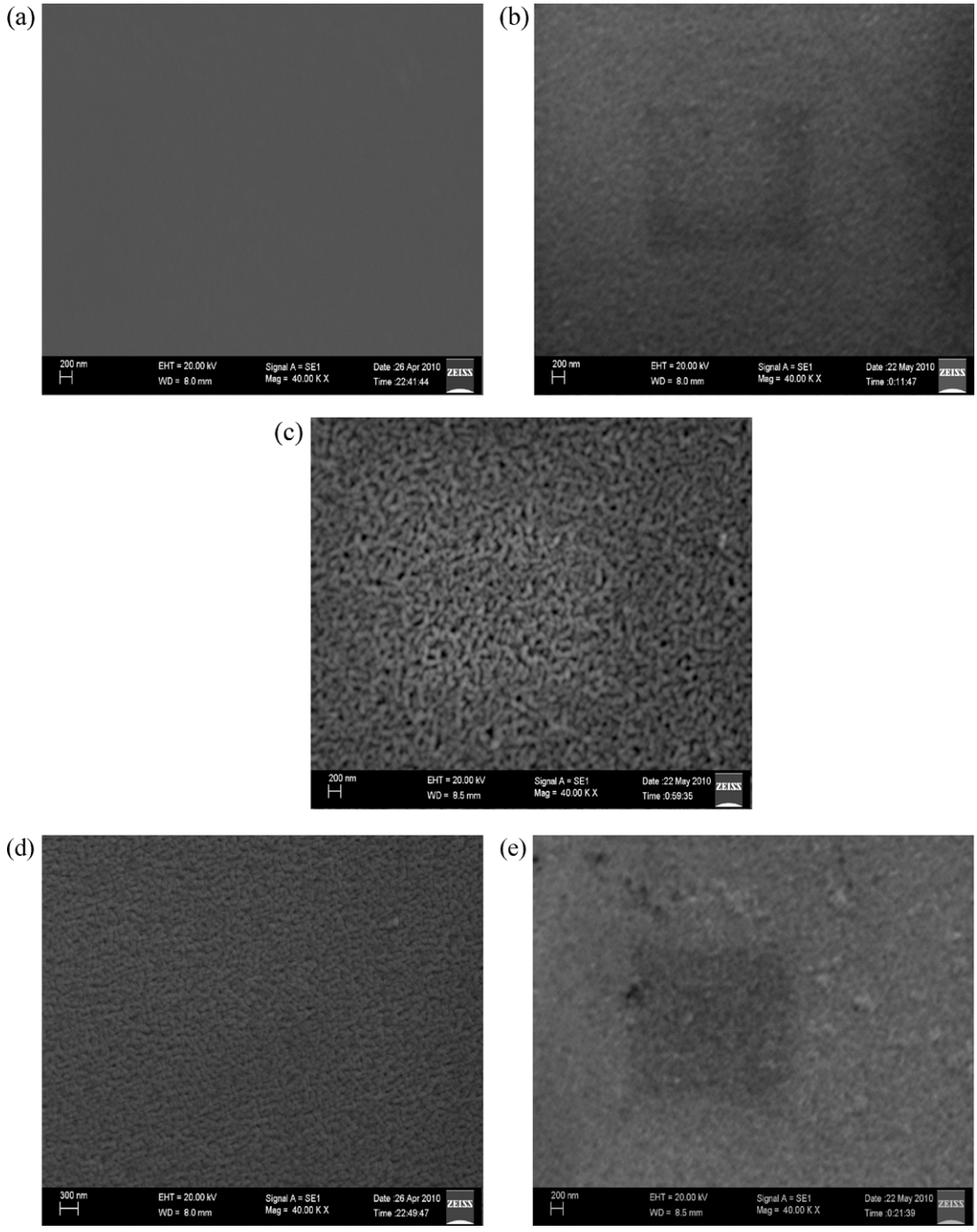

Fig. 3. SEM images of NiO films as a function of oxygen partial pressure (a) 2×10^{-2} Pa (b) 4×10^{-2} Pa (c) 6×10^{-2} Pa (d) 8×10^{-2} Pa (e) 10×10^{-2} Pa.

content of nickel was decreased as oxygen partial pressure increased.

3.4. Optical properties

The optical transmittance of the films increased from 45% to 60% with increasing of oxygen partial pressure from 2×10^{-2} to 6×10^{-2} Pa. On further increasing the oxygen partial pressure to 10×10^{-2} Pa, the transmittance of the films decreased to 43% (Table 4). It was observed that the absorption edge was shifted towards shorter wavelength side with the increase of oxygen partial pressure up to 6×10^{-2} Pa, which is correlated with the change in the optical band gap. As the amount of oxygen partial pressure increases, the transmittance of films increases, which may be due to the decrease of oxygen vacancies.

The optical band gap of the films increased from 3.65 to 3.82 eV with the increase of oxygen partial pressure from 2×10^{-2} to 6×10^{-2} Pa, beyond this oxygen partial pressure the optical band gap of NiO films was decreased to 3.69 eV. The

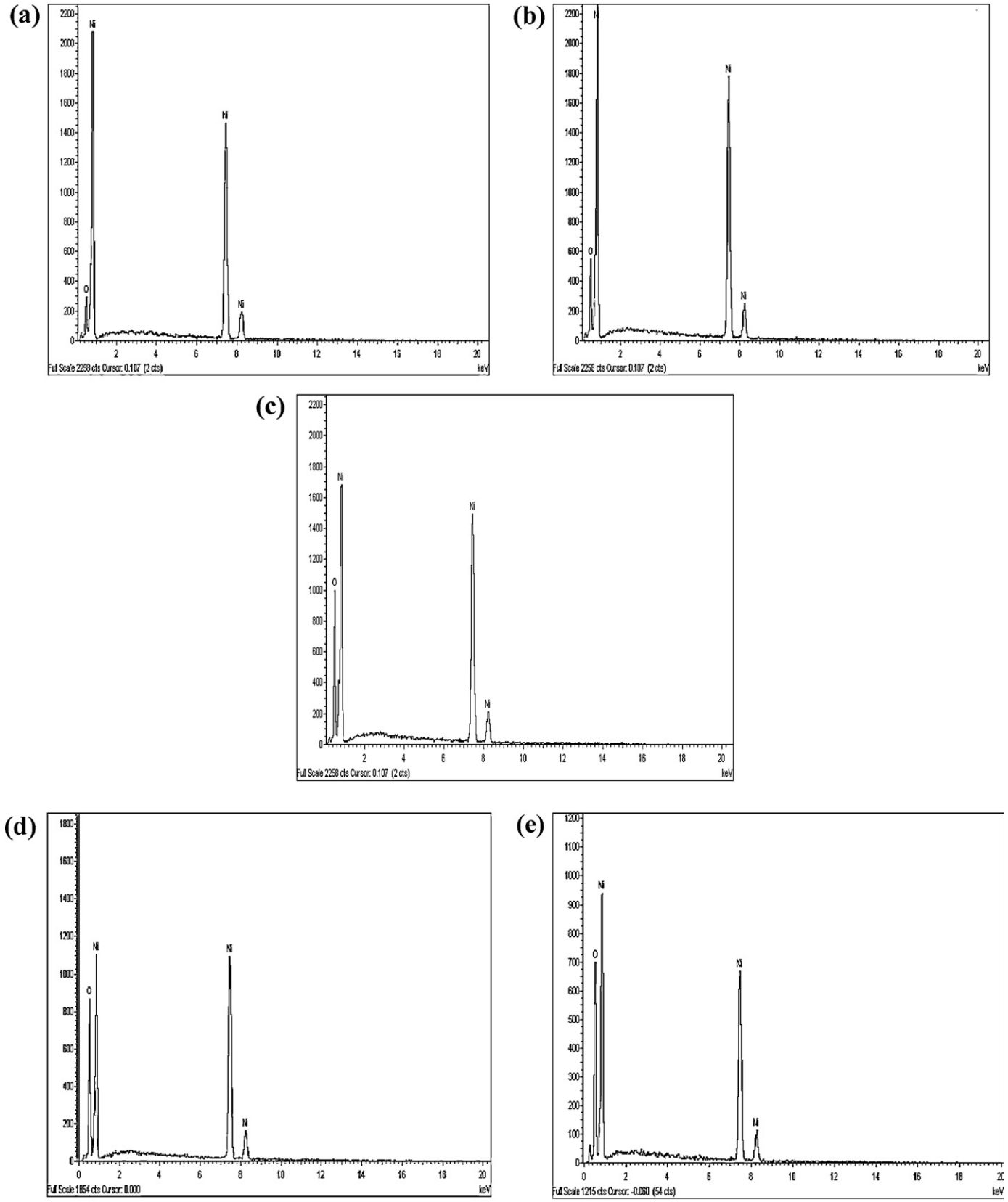

Fig. 4. EDS images of NiO films as a function of oxygen partial pressure (a) 2×10^{-2} Pa (b) 4×10^{-2} Pa (c) 6×10^{-2} Pa (d) 8×10^{-2} Pa (e) 10×10^{-2} Pa.

Table 3
The compositional analysis of dc reactive magnetron sputtered NiO films at various sputtering pressures by Energy Dispersive Spectroscopy (EDS).

Oxygen partial pressure (Pa)	Element	Weight %	Atomic %	Ni/O
2×10^{-2}	O K	12.80	34.99	1.86
	Ni K	87.20	65.01	
4×10^{-2}	O K	15.84	40.87	1.47
	Ni K	84.16	59.13	
6×10^{-2}	O K	20.78	49.04	1.04
	Ni K	79.22	50.96	
8×10^{-2}	O K	24.53	54.40	0.84
	Ni K	75.47	45.60	
10×10^{-2}	O K	28.76	59.70	0.67
	Ni K	71.24	40.30	

Table 4
Optical information of dc reactive magnetron sputtered NiO films at various oxygen partial pressures.

Oxygen partial pressure (Pa)	Transmittance (%)	Optical band gap (eV)
2×10^{-2}	45	3.65
4×10^{-2}	50	3.74
6×10^{-2}	60	3.82
8×10^{-2}	56	3.79
10×10^{-2}	43	3.69

optical band gap obtained at an oxygen partial pressure of 6×10^{-2} Pa in the present investigation was in good agreement with the reported value of rf magnetron sputtered NiO films at 523 K by Nandy et al. [25]. However in the literature large optical band gap of 4.3 eV was reported by Romero et al. [26] in chemical spray pyrolysis deposited NiO films. Varkey and Fort [27] reported the lower energy gap of 3.25 eV for NiO films coated using solution growth method.

From the FTIR studies it was observed that all the samples were humidity free and exhibits the absorption band around 500 cm^{-1}, this may be due to the stretching vibration of Ni–O bond of nickel oxide. Fig. 5 shows the FTIR transmission spectrum of NiO film deposited at an oxygen partial pressure of 6×10^{-2} Pa.

3.5. Electrical properties

The electrical properties of the films were highly influenced by oxygen partial pressure. Fig. 6 shows the electrical resistivity of NiO films as a function of oxygen partial pressures. It was found that the resistivity of the NiO films decreases from 85.4 to 5.1 Ωcm with the increase of oxygen partial pressure from 2×10^{-2} to 6×10^{-2} Pa, and then increased to 47.3 Ωcm at higher oxygen partial pressure of 10×10^{-2} Pa. The decrease in resistivity with the oxygen partial pressure was related to increase in hole concentration and crystallinity of the films. On the other hand the carrier concentration of the films increased from 6.0×10^{16} to 2.6×10^{17} cm^{-3} with the increase of oxygen partial pressure

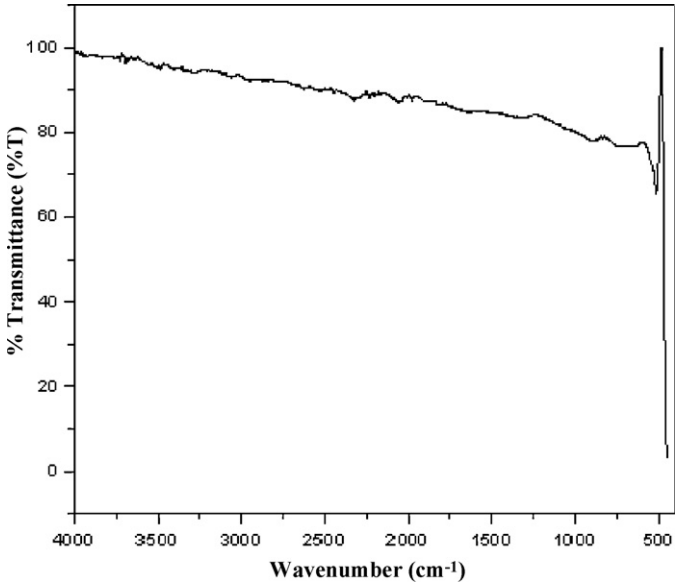

Fig. 5. FTIR Spectrum of NiO film deposited at oxygen partial pressure of 6×10^{-2} Pa.

from 2×10^{-2} to 6×10^{-2} Pa. The increase in hole concentration with the oxygen partial pressure may be attributed to increase in shallow acceptor states such as nickel vacancies and/or interstitial oxygen, resulting from enhanced oxidization during the sputter deposition [2]. The Hall mobility measurements indicated that the films were p-type conduction. The Hall mobility of the films increased from 1.2 to 4.6 $cm^2\ V^{-1}\ s^{-1}$ with the increase of oxygen partial pressure from 2×10^{-2} to 6×10^{-2} Pa, thereafter it decreased to 2.7 $cm^2\ V^{-1}\ s^{-1}$ at higher oxygen partial pressures. The low mobility of the films grown under high oxygen pressure is believed to be due to collisional energy loss of the particles with oxygen during their arrival towards the substrate surface [28]. This energy loss considerably reduces the surface mobility

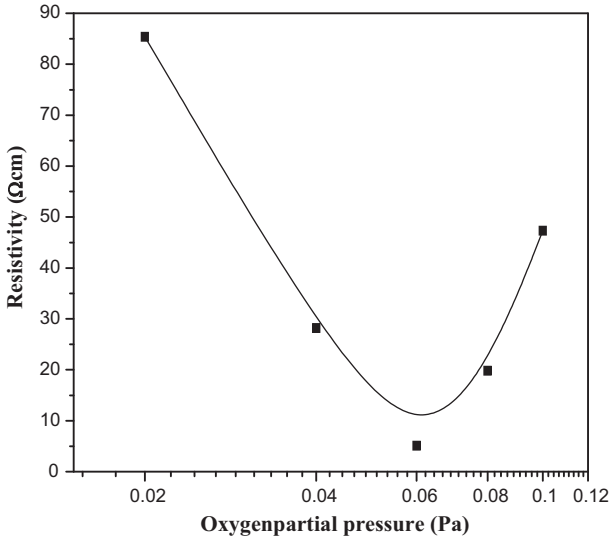

Fig. 6. Variation of electrical resistivity of NiO films as a function of oxygen partial pressure.

Table 5
Hall effect data of dc reactive magnetron sputtered NiO films at different oxygen partial pressures.

pO_2 (Pa)	Resistivity (Ω cm)	Carrier concentration (cm^{-3})	Mobility ($cm^2\ V^{-1}\ s^{-1}$)
2×10^{-2}	85.40	6.0×10^{16}	1.2
4×10^{-2}	28.20	8.8×10^{16}	2.5
6×10^{-2}	05.10	2.6×10^{17}	4.6
8×10^{-2}	19.80	7.8×10^{16}	4.0
10×10^{-2}	47.30	4.9×10^{16}	2.7

which gradually impairs the crystal quality. The detailed Hall effect data was listed in Table 5.

4. Conclusions

NiO films were grown by dc reactive magnetron sputtering and properties were investigated as a function of the oxygen partial pressure. XRD results revealed that the orientation of the films was strongly influenced by the oxygen partial pressure. The lattice parameter of the films varied from 0.4202 to 0.4189 nm with increase of oxygen partial pressure from 4×10^{-2} to 6×10^{-2} Pa. The electrical resistivity of the films decreased with increase of oxygen partial pressure up to 6×10^{-2} Pa. The optical transmittance of the films was increased from 45 to 60% and optical band gap of the films increased from 3.65 to 3.82 eV with increasing of oxygen partial pressure from 2×10^{-2} to 6×10^{-2} Pa, thereafter optical band gap decreased to 3.69 eV on further increasing the oxygen partial pressure to 10×10^{-2} Pa.

References

[1] H.J.M. Swagten, G.J. Strijkers, P.J.H. Bloemen, M.M.H. Willekens, W.J.M. De Jonge, Phys. Rev. B 53 (1996) 9108–9114.
[2] H. Sato, T. Minami, S. Takata, T. Yamada, Thin Solid Films 236 (1993) 27–31.
[3] M.J. Carey, A.E. Berkowitz, J. Appl. Phys. 73 (1993) 6892–6897.
[4] S. Soeya, H. Hoshiya, K. Meguro, H. Fukui, Appl. Phys. Lett. 71 (1997) 3424–3426.
[5] D.G. Hwang, S.S. Lee, C.M. Park, Appl. Phys. Lett. 72 (1998) 2162–2164.
[6] S. Koide, J. Phys. Soc. 20 (1965) 123–131.
[7] I. Hotovy, J. Huran, P. Siciliano, S. Capone, L. Spiess, V. Rehacek, Sens. Actuators B: Chem. 78 (2001) 126–132.
[8] H. Kumagai, M. Matsumoto, K. Toyoda, M. Obara, J. Mater. Sci. Lett. 15 (1996) 1081–1083.
[9] M. Kitao, K. Izawa, K. Urabe, T. Komatsu, S. Kuwano, S. Yamada, Jpn. J. Appl. Phys. 33 (1994) 6656–6662.
[10] S. Nishizawa, T. Tsurumi, H. Hyodo, Y. Ishibashi, N. Ohashi, O. Ya-mane Fukunaga, Thin Solid Films 302 (1997) 133–139.
[11] G.H. Yu, L.R. Zen, F.W. Zhu, C.L. Chai, W.Y. Lai, J. Appl. Phys. 90 (2001) 4039–4043.
[12] W.C. Yeh, M. Matsumura, Jpn. J. Appl. Phys. 36 (1997) 6884–6887.
[13] M. Tanaka, M. Mukai, Y. Fujimori, M. Kondoh, Y. Tasaka, H. Baba, S. Usami, Thin Solid Films 281 (1982) 453–456.
[14] S.A. Ali, S.A. Mahmoud, M. Abdel-Rahman, K. Abdel-Hady, Egyptian J. Solids 1 (1998) 5.
[15] S.A. Mahmoud, S.A. Ali, M. Abdel-Rahman, K. Abdel-Hady, Physica B 293 (2000) 125–131.
[16] L. Wang, Z. Zhang, Y. Cao, J. Ceram. Soc. Jpn. 101 (1993) 227.
[17] S.A. Mahmoud, A.A. Akl, H. Kamal, K.A. Hady, Physica B 311 (2002) 366–375.
[18] L.J. van der Pauw, Philips Res. Rep. 13 (1958) 1–9.
[19] A. Sivasankar Reddy, G. Venkata Rao, S. Uthanna, P. Sreedhara Reddy, Mater. Lett. 60 (2006) 1617–1621.
[20] J.W. Lee, I.H. Park, C.W. Chung, Integr. Ferroelectr. 74 (2005) 71–77.
[21] E. Fujji, A. Tomozawa, H. Torii, R. Takayama, Jpn. J. Appl. Phys 35 (1996) L328–L330.
[22] M. Ohring, The Material Science of Thin Solid Films, Academic Press, New York, 1992.
[23] W. Buckel, J. Vac. Sci. Technol. A 6 (1969) 606.
[24] M. Adamik, P.B. Barna, I. Tomov, D. Biro, Phys. Status Solidi A 145 (1994) 275–281.
[25] S. Nandy, U.N. Maiti, C.K. Ghosh, K.K. Chattopadhyay, J. Phys. Condens. Matter 21 (2009) 15804 (7 pp.).
[26] R. Romero, F. Martin, J.R. Ramos-Barrado, D. Leinen, Thin Solid Films 518 (2010) 4499–4502.
[27] A.J. Varkey, A.F. Fort, Thin Solid Films 235 (1993) 47–50.
[28] T.K. Yong, T.Y. Tou, B.S. Teo, Appl. Surf. Sci. 248 (2005) 388–391.